Chemical and phase chemical characterisation of three different tap-hole clays

I.C. Thobadi[a,b*], M. Mnisi[a], J.D. Steenkamp[a,b], E Matinde[a,b], and W. Clark[c]

[a]*Pyrometallurgy Division, MINTEK, Randburg, 2125, South Africa*
[b]*Department of Chemical and Metallurgical Engineering, University of the Witwatersrand, Johannesburg, 0001, South Africa*
[c]*Mineralogy Division, MINTEK, Randburg, 2125, South Africa*
**Corresponding author: itumelengt@mintek.co.za*

ABSTRACT

Pyrometallurgical smelters utilise tap-holes, through which liquid metal, matte and/or slag are tapped at regular intervals. However, tap-hole failures can have a devastating impact on smelters, which includes loss of equipment, human life and business interruptions. Contributing factors to tap-hole failures include poor and/or incorrect refractory material selection, including tap-hole clays. The functions of tap-hole clays in smelters include their ability to be extruded and drilled with ease at the end and beginning of a tap, and their ability to resist chemical wear due to molten metal and slag during tapping. Mintek is currently developing methods of evaluating properties of tap-hole clays with a specific focus on workability, and wear mechanisms of clays due to ferrochrome alloy and slag. Of particular interest to this study was the characterisation of various tap-hole clays.

This paper evaluates the chemical and phase chemical properties of three different tap-hole clays. The bulk chemical composition of the tap-hole clays was determined by inductively coupled plasma optical emission spectroscopy, proximate analyses and combustion methods. The bulk phase compositions and specific phase chemical compositions were studied using quantitative X-ray diffraction, scanning electron microscope and electron probe microanalyses techniques.

Keywords: Tap-hole clay, chemical analyses, phase chemical analyses, ferrochrome

1. Introduction

Clays are naturally occurring materials composed primarily of fine-grained minerals (Guggenheim 1995). They are generally plastic at appropriate water contents and will harden when fired or dried. The minerals commonly found in clays are silicates of less than 2 microns in size (Schulze 2005; Guggenheim and Martin 1995; Heckroodt 1991).

Clays have found widespread applications in various industries such as pharmaceuticals and ceramics, including in the pyrometallurgy industry (Guggenheim and Martin 1995).

The function of tap-hole clays in pyrometallurgy furnaces is not only to sufficiently plug the tap-hole between taps, but also to ensure that the tap-hole can be drilled with ease at subsequent taps. Some of the properties required for good a tap-hole clay to sufficiently perform these functions include (Heckroodt 1991; Nelson and Hundermark 2014) : (1) optimal workability, which is the ability of the clay to be charged and drilled with ease, (2) high wear and corrosion resistance , i.e. the ability of the clay to resist erosion due to hot alloy and slag and therefore to reduce tap-hole area wear, (3) good sinterability, which is the ability of the clay to cure to the required strength without shrinkage, and (4) adhesive strength, which is the ability to provide a tight seal within the tap-hole, required for proper adhering of new tap-hole mix to old tap-hole mix and/or tap-block refractory.

Historically, tap-hole clay materials used in the pyrometallurgy industry, were sourced from naturally occurring clays. Whilst crude clay is still being used in some smelting operations, there has been a shift by most operations to utilise beneficiated tap-hole clays in which impurities have been removed and the composition (e.g. binders and aggregates) is designed to meet the specific property requirements (Nightingale *et al* . 2006). Water, phenolic resins, tar, and various oils are typically used as binders in various clay formulations (Dash 2009). The function of a binder is to improve the plasticity properties, which in turn directly influences the workability and binding properties of the clay (Dash 2009). Corundum and quartz are some of the materials added in the refractory aggregate to provide resistance to chemical attack (Dash 2009; Nightingale *et al* . 2006). Silicon carbide (SiC) and nitride (Si_3N_4) additives are added to the clay to impart corrosion and abrasion resistance, and to improve sinterability of the clay (Nelson and Hundermark 2014).

In addition to corrosion and abrasion resistance, tap-hole clays must have low porosity and a dense structure at high temperatures in order to minimise the potential for chemical attack by alloy and slag (Heckroodt 1991). The porosity of the clay after plugging into the tap-hole is influenced by the portion of the volatile materials in the binder. In essence, high volatile and combustible matter in the binder results in high porosity of the clay. The bigger the pores or cracks in the plugged clay, the easier it is for the alloy and slag to penetrate through the pores thus attacking the clay (Heckroodt 1991). This means that the characterization of different clays is important in order to create a basis for evaluating the impact of the chemical and phase chemical properties of clays on their performance in the aforementioned functions.

The broad objective of this research was to determine the chemical and phase chemical compositions of three (selected) tap-hole clays. The research question addressed in the study was: "which chemical and phase chemical properties describe each of the 3 tap-hole clays?" The data gathered will be used in a follow up study which will evaluate the impact of chemical and phase chemical analyses, on the functions of tap-hole clays in ferrochrome smelting operations.

The actions undertaken during the study included 1) sourcing of clays from different suppliers, 2) preparing clays for characterization, and 3) characterising the clays by determining their bulk chemical, bulk phase chemical, and specific phase chemical compositions.

2. Experimental

2.1. Sourcing tap-hole clay

Three different industrial tap-hole clays were sourced from three different suppliers and are referred to as Clay A, Clay B, and Clay C in this paper. The tap-hole clays selected for this study varied significantly in terms of their aggregate composition and the binder phases used in their respective mixtures. Clay A was an experimental clay with no datasheet available and was bound with coal tar pitch. Clay B and Clay C were commercial clays currently in use at a local ferrochrome smelter. According to the product datasheets, clay B was resin and water-bonded, with mainly SiO_2 in the aggregate. Clay C was tar and resin bonded, with similar amounts of Al_2O_3 and SiO_2 as aggregate.

2.2. Preparing samples

Clay samples were prepared using the pilot-scale drill and clay-gun presented in Figure 1 (a). The extrusion allowed for the preparation of more compacted samples. It was postulated that compacting the sample using the clay-gun equipment will homogenise the samples better than the as-received material. The clay-gun barrel was filled with 11 – 17 kg of clay, depending on the type of clay. The clay-was extruded onto an angle-iron attached to the 65 mm diameter nozzle of the clay-gun. The extruded clay was cut into sections for subsequent characterization. Figure 1 (b) shows Clay C samples prepared for characterization. Clay A immediately lost the cylindrical shape after being extruded and this was attributed to sample characteristics, which is the subject of the current study.

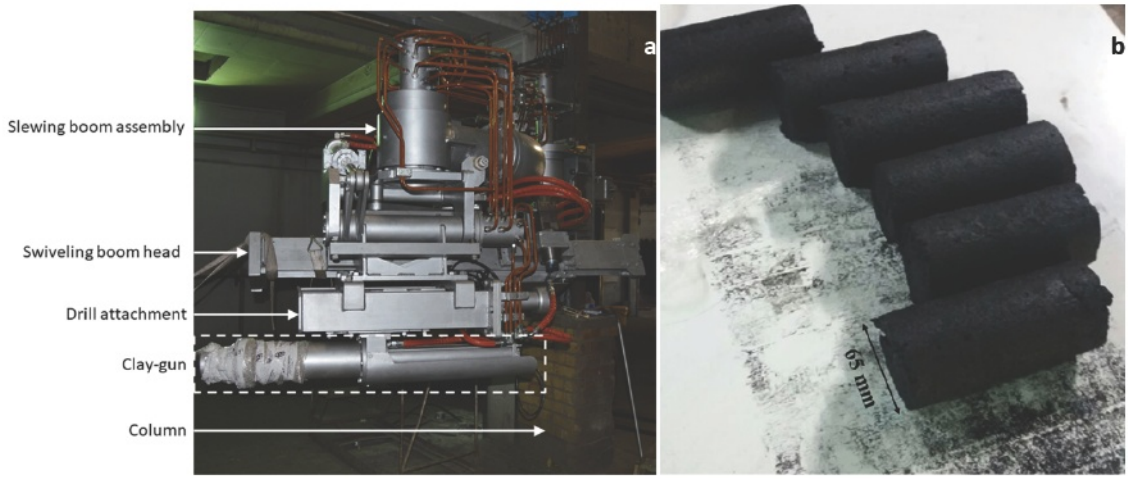

Fig. 1. a) Pilot-scale drill and clay-gun, and b) Clay C samples prepared using the drill and mudgun, 65 mm diameter.

2.3. Characterizing tap-hole clay samples

The chemical compositions of the clays were determined using proximate analyses and other bulk chemical analyses methods. Bulk phase chemical and specific phase chemical compositions of the clays were determined by X-ray diffraction (XRD), scanning electron microscopy (SEM) with energy dispersive spectroscopy (EDS), and electron probe microanalyses (EPMA).

2.3.1. Chemical analyses

Chemical analyses was determined on "as-extruded" clays as well as after drying to evaluate if removal of moisture influenced the chemical compositions of the clays. Some of the samples from each clay were analysed "as extruded", and other samples were dried in an oven at 150°C for 24 hours (ASTM-D3173 2011). Proximate analyses techniques (similar to coal analyses) (ASTM-D3172 2013), were applied in order to determine the inherent moisture (ASTM-D3173 2011), ash (ASTM-D3174 2012), and volatile matter content (ASTM-D3175 2011) of the samples, and to calculate the fixed carbon contents by difference. The bulk chemical compositions of the as-extruded and dried samples were determined by Inductively Coupled Plasma (ICP) methods.

2.3.2. Bulk phase chemical analyses

Bulk phase analyses was conducted on "as-extruded" clays. Representative particulate sub-samples were analysed using quantitative XRD to obtain the bulk mineralogical assemblage. A Bruker D8 Advance powder diffractometer, with Linxeye detector and Co-Kα radiation was employed. The phases were identified using Bruker EVA® software and quantified using the TOPAS® software. Quantitative XRD involves the identification of mineral phases and their total contribution in the sample measured by mass %. XRD typically only identifies crystalline minerals/phase that are present in amounts of >1 mass % in the sample. Amorphous phases cannot be identified with the technique described.

2.3.3. Specific phase chemical analyses

To determine the specific phase chemical compositions, representative samples of the clay samples were prepared into polished sections for analyses using the SEM. The Zeiss Evo MA15 SEM equipped with a Bruker EDS was used to analyse the phase composition of the clays. The SEM analyses was undertaken to describe the phases present in the clay and their textural relationships with other minerals in each of the samples. Backscattered electron (BSE) micrographs supplemented by element maps and EDS were used to interpret mineral chemistry of individual particles/phases.

Element maps were generated by measuring the characteristic X-Ray intensity of chemical elements relative to their lateral position on the sample. Variations in X-Ray intensity indicated the relative concentration of the specific element across the recorded field of view. One or more maps were recorded simultaneously using image brightness intensity as a function of the local relative concentration of the elements present. Areas containing concentrations of elements were thus documented and, in

combinations with different elements displayed in false colour, highlighted the presence of different phases.

The EPMA was used to determine the elemental composition of phases present. Analyses was carried out using Wavelength Dispersive Spectrometry (WDS) on the Electron Probe Microanalyser. Counting times of 10 seconds on peak and 5 seconds on each of the two background positions adjacent to the peak, are employed at an accelerating voltage of 20 kV, a beam current of 30 nA with a beam defocussed to a diameter of 5 µm. The system is calibrated using matrix matched standards.

3. Results

3.1. Chemical analyses

The results for the proximate analyses and ICP-OES analyses are presented in Table 1 and Table 2. The A/C ratio in Table 1 is the ratio of *Ash* to the sum of *Volatile matter* and calculated *Fixed carbon* as indicated in equation 3.1.1. The A/S ratio in Table 2 is the ratio of Al_2O_3 to SiO_2 as indicated in equation 3.2.2.

$$A/C = \frac{Ash}{Volatile\ matter + Fixed\ carbon} \quad 3.1.1$$

$$A/S = \frac{Al_2O_3}{SiO_2} \quad 3.1.2$$

Table 1.

Proximate analyses of as-extruded and dried clay samples. Results are presented in mass percent.

Methods	***As-extruded***			***Dried at 150°C***		
	Clay A	**Clay B**	**Clay C**	**Clay A**	**Clay B**	**Clay C**
Inherent moisture	0.73	0.61	0.38	0.78	1.05	0.58
Ash (dry basis)	49.45	76.50	90.85	51.20	77.93	90.60
Volatile matter (dry basis)	11.87	8.31	7.27	13.70	10.18	7.15
Fixed carbon (dry basis)	37.96	14.59	1.51	34.33	10.85	1.67
Total	100	100	100	100	100	100
A/C ratio	0.99	3.34	10.35	1.07	3.71	10.27

Table 2.

Normalised ICP-OES analyses of the ash of as-extruded and dried clay samples. Results presented in mass percent.

Methods	***As-extruded***			***Dried at 150°C***		
	Clay A	**Clay B**	**Clay C**	**Clay A**	**Clay B**	**Clay C**
Al_2O_3	44.7	6.5	54.2	44.4	6.3	56.1
SiO_2	48.5	89.1	42.2	45.2	90.4	40.2
CaO	1.2	1.3	0.7	0.2	0.9	0.0
Fe_2O_3	3.2	2.6	1.8	5.2	1.9	1.7
TiO_2	0.2	0.3	0.2	0.2	0.3	0.2
K_2O	1.2	0.1	0.3	4.7	0.1	1.7

Na_2O	1.0	0.1	0.6	0.2	0.1	0.1
Total	100.0	100.0	100.0	100.0	100.0	100.0
$Al_2O_3 + SiO_2$	93.2	95.6	96.4	89.6	96.7	96.3
A/S ratio	0.9	0.1	1.3	1.0	0.1	1.4

3.2. Bulk phase chemical analyses

Table 3 presents the bulk phase composition of the three tap-hole clays before removal of moisture.

Table 3.

Bulk phase composition of the clays in mass percent

Mineral	***Chemical formulae***	***Clay A***	***Clay B***	***Clay C***
Andalusite	Al_2SiO_5	83.5	-	87
Quartz	SiO_2	3.5	92.5	6.5
Clay/illite/mica	$KMg_3AlSi_3O_{10}(OH)_2$	12	3	6.5
Portlandite	$Ca(OH)_2$	1	1.5	-
Anorthite	$CaAl_2Si_2O_8$	-	3	-
Total		100	100	100

3.3. Specific phase chemical analyses

Figures 2-4 present the BSE micrographs for Clay A, Clay B, and Clay C. The specific phase chemical compositions of the main phases were identified by EDS and quantified with EPMA. The specific phase chemical analyses for Clay A, Clay B and Clay C are presented in Table 4, Table 5 and Table 6 respectively.

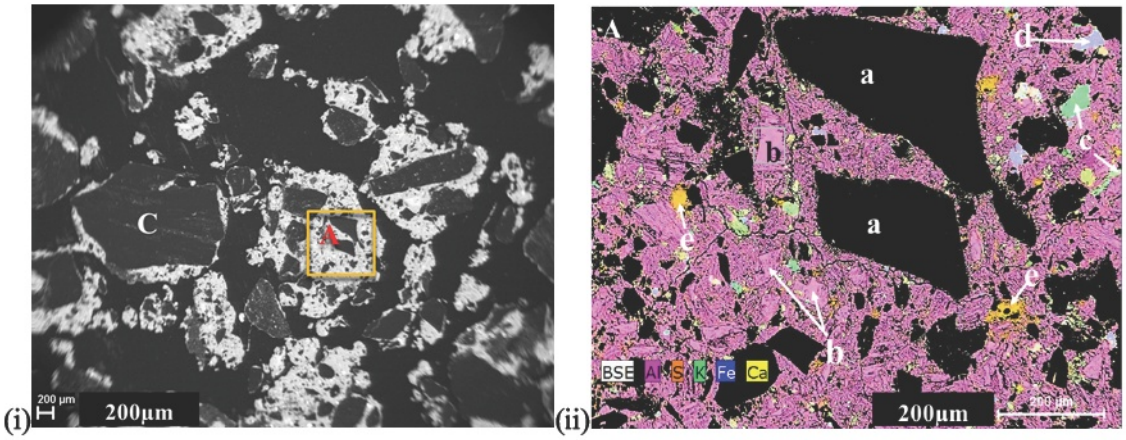

Fig. 2. (i) BSE micrograph of Clay A. C denotes graphite/carbon particles and A the area presented in (ii) BSE/Xray map composite micrograph showing (a) graphite/carbon, (b) andalusite, (c) mica/clay minerals, (d) Fe-oxide, (e) gypsum/lime. Both scale bars indicate 200µm.

Table 4.

Normalised compositions of phases in Clay A phases as determined by EDS and EPMA. Single point analyses is reported for some phases and averages of multiple point analyses were reported for other phases. Results presented in mass percent.

		Points	*O*	*Na*	*Mg*	*Al*	*Si*	*P*	*S*	*K*	*Ca*	*Fe*	*Total*
Andalusite	EDS		49.25	-	-	34.55	16.20	-	-	-	-	-	100.00
	EPMA	10	48.41	0.02	0.03	33.02	15.74	0.01	0.01	0.02	2.40	0.35	100.00
Quartz	EDS	*	*	*	*	*	*	*	*	*	*	*	0.00
	EPMA	2	52.57	0.01	0.16	3.04	43.52	0.01	0.00	0.47	0.00	0.21	100.00
Mica/Clay	EDS	1	39.24	-	3.66	12.23	15.43	-	-	7.92	1.53	19.98	100.00
	EPMA	1	39.04	0.12	3.12	10.73	16.91	0.04	0.05	7.19	0.04	22.77	100.00
Fe-oxide	EDS	3	22.81	-	-	0.48	0.47	-	-	-	-	75.78	100.00
	EPMA	2	26.48	0.21	0.28	1.32	4.85	0.20	0.16	1.36	0.63	64.50	100.00
Lime/	EDS		43.79	-	-	0.85	1.22	-	18.38	0.73	35.03	-	100.00
Gypsum	EPMA		*	*	*	*	*	*	*	*	*	*	0.00

non-detected elements -

analyses not available *

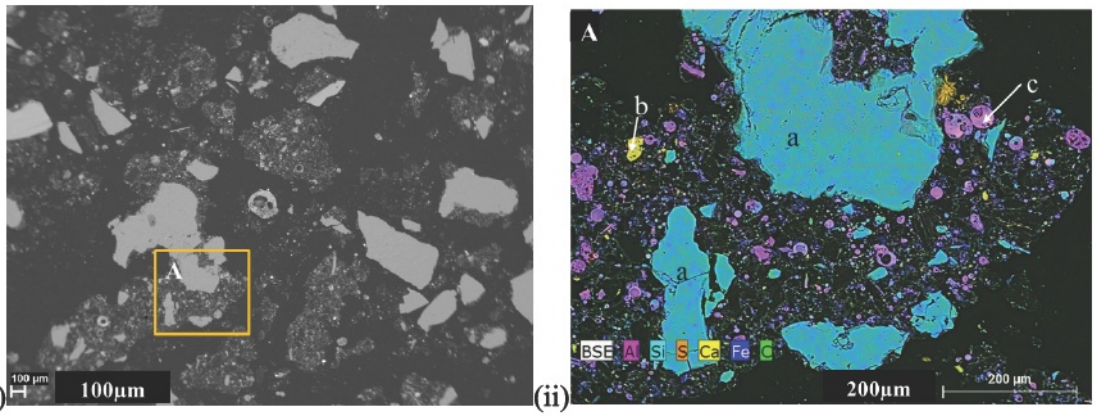

(i) (ii)

Fig .3. (i) BSE micrograph of Clay B (ii) BSE/Xray map composite micrograph of clay B (a) quartz, (b) lime/portlandite, (c) mullite.

Table 5.

Normalised compositions of phases in Clay B phases as determined by EDS and EPMA. Averages of multiple point analyses were reported for the phases results presented in mass percent.

		Points	*O*	*Na*	*Mg*	*Al*	*Si*	*P*	*S*	*K*	*Ca*	*Fe*	*Total*
Quartz	EDS	2	52.61	-	0.21	1.99	44.28	-	-	-	-	0.46	100.00
	EPMA	4	53.02	0.01	0.06	0.83	45.78	0.00	0.00	0.09	0.05	0.18	100.00
Mullite/Clay	EDS	2	48.92	-	0.519	21.44	23.94	0.21	-	0.36	1.77	2.21	100.00
	EPMA	7	44.02	0.21	0.34	17.53	23.35	0.05	0.02	1.99	2.07	0.71	100.00
Lime/portlandite	EDS	2	28.62	-	0.28	0.05	0.07	-	0.12	-	69.44	-	100.00
	EPMA	3	29.09	0.03	0.57	0.44	0.48	0.01	0.12	0.02	68.64	0.60	100.00

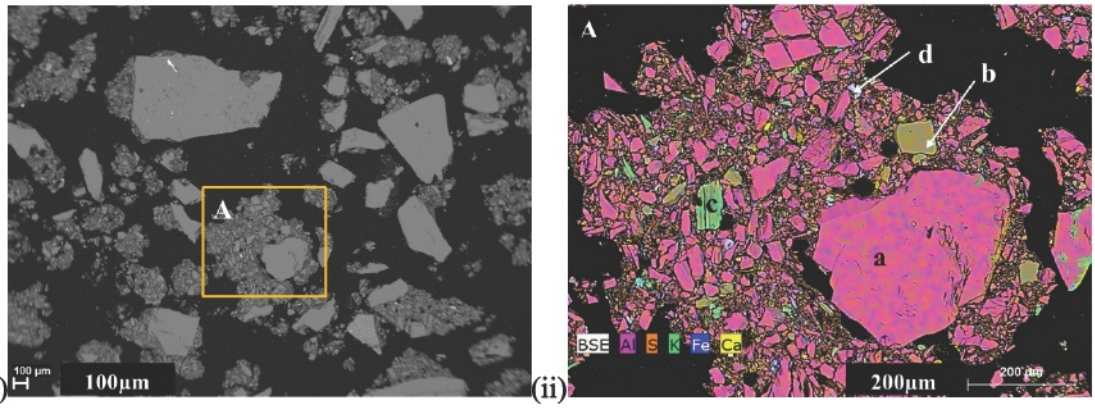

Fig. 4. (i) BSE micrograph of Clay C (ii) BSE/Xray map composite micrograph of Clay C at higher magnification (a) andalusite, (b) quartz, (c) mica/clay minerals, (d) Fe-oxide

Table 6.

Normalised compositions of phases in Clay C phases as determined by EDS and EPMA. Single point analyses is reported for some phases and averages of multiple point analyses were reported for other phases. Results presented in mass percent.

		Points	*O*	*Na*	*Mg*	*Al*	*Si*	*P*	*S*	*K*	*Ca*	*Fe*	*Total*
Andalusite	EDS	2	49.03	-	-	34.48	16.09	-	-	-	-	-	100.0(
	EPMA	10	49.14	0.06	0.04	33.90	16.51	0.00	0.02	0.02	0.00	0.30	100.0(
Quartz	EDS	1	53.16	-	0.07	0.31	46.36	-	-	0.08	-	0.03	100.0(
	EPMA	5	53.24	0.00	0.00	0.03	46.67	0.01	0.00	0.00	0.01	0.03	100.0(
Mica/Clay	EDS	1	46.13	0.91	0.72	21.41	21.31	-	-	8.76	-	0.76	100.0(
	EPMA	4	47.84	0.86	0.18	22.34	22.60	0.11	0.05	3.63	1.47	0.92	100.0(
Fe-oxide	EDS	1	25.75	-	-	2.33	2.45	0.49	3.78	-	0.51	64.69	100.0(
	EPMA	*	*	*	*	*	*	*	*	*	*	*	0.00

4. Discussion

4.1. Chemical analyses

As indicated in Table 1, the proximate analyses of the clays indicated that Clay A contained the lowest amount of inorganic material as indicated by the *ash content* at 49.5%. It also contained the highest amount of solid combustible component as indicated by the *calculated fixed carbon* at 38.0%. Clay C contained the highest amount of ash content and the lowest amount of calculated fixed carbon, at 90.9% and 1.5% respectively. The results for Clay B were in-between with 76.5% ash content and 14.6% calculated fixed carbon. The calculated fixed carbon does not include carbon associated with the volatile matter in the clay which includes binder material additives i.e.tar and resin which are reported in the material datasheets. The volatile matter for Clay A, Clay B and Clay C was 11.9%, 8.3% and 7.3%, respectively. The clays did not contain significant amounts of moisture, with clay A, Clay B and Clay C containing 0.7%, 0.6% and 0.4% moisture respectively. As a result the bulk chemical analyses of the clays as-extruded were comparable to that of the clays after drying. Volatile matter and fixed

carbon are the main components of the clays which are expected to have an impact on functions of the clay upon heating. The impact of moisture removal will be minimal due to the low moisture contents of the three clays.

Removal of volatile matter upon heating of the clays will result in pores in the clay. Furthermore, Clay A with the lowest A/C-ratio (highest fixed carbon of all three clays), will result in even more pores upon heating during applications in a tap-hole. Porosity in the heated clay could result in a clay plug that can be drilled more easily. Porosity could lead to infiltration of molten material in the clay creating potential for chemical wear or difficulty with drilling. These theories will be tested in future work. On the other hand, as highlighted in section 2.2, Clay A did not retain its shape during extrusion, which could present challenges during tap-hole closure. Studies on the workability of tap-hole clays shed more light on the matter (Steenkamp, 2018).

From the ICP-OES analyses in Table 2, the inorganic components for all three clays consist of more than 90% Al_2O_3 + SiO_2. Clay A and Clay C contained significant amounts of Al_2O_3 as indicated by their A/S ratios being 0.9 and 1.3 respectively, Clay C predominantly consists of SiO_2 with an A/S ratio of 0.1. The variation in the bulk compositions of the clays and the compositions of the inorganic material present potential for different chemical interactions with molten material when they are used as tap-hole clay.

4.2. Bulk phases chemical analyses

The bulk phase chemical analyses were conducted on "as extruded" clays due to the minimal moisture detected using proximate analyses methods. The analyses in Table 3 indicated that Andalusite is the dominant crystalline phase in Clay A and Clay C, which explains the high A/S-ratios in Table 3. The main difference between Clay A and Clay C is the clay (mica) mineral content, which was higher for Clay A, i.e. 12% compared to 6.5% present in Clay C. In Clay B the dominant crystalline phase was quartz. Other minerals identified in Clay B included the mica, portlandite, and anorthite. Andalusite was not detected in Clay B.

4.3. Specific phase chemical analyses

The specific phase analyses were also conducted on "as extruded" clays. The analyses of the clays is presented in the SEM images in Figures 2 to 4 and the associated EDS analyses Tables 4 to 6. EPMA analyses was conducted to validate the EDS analyses and is also included in Tables 4 to 6. Figure 2 and Table 4 confirmed the presence of andalusite in Clay A. Other minerals phases identified were the clay mineral (mica), and quartz. Clay A was also characterised by abundant carbon present in sizes ranging between 1 µm to over 500 µm. The coarser aggregate material (carbon and andalusite) in Clay A were bonded by a fine mixture of andalusite, mica, and quartz. Figure 3 and Table 5 demonstrated the presence of quartz, mica and portlandite in Clay B. Quartz is present in sizes ranging from 10 µm to 600 µm. The coarser quartz particles were bonded by a fine mixture of finer quartz, mica, portlandite, and fine carbon particles. Figure 4 and Table 6 demonstrated that the dominant phase present in the Clay C was

andalusite. The andalusite minerals occurred in sizes ranging from 10 µm to 2500 µm. The coarser andalusite aggregate particles were bonded by a fine mixture of fine grained particles of andalusite and quartz, and mica. All three clays contain organic material binders which were not analyzed using the phase chemical and specific phase chemical analyses methods employed in this study.

5. Conclusions

The focus of this study was to investigate the chemical, bulk phase chemical and specific phase chemical compositions of three tap-hole clays. These clays were selected to investigate the impact of various clays with different properties on their functions in ferrochrome smelting. The three tap-hole clays were found to contain various inorganic and organic components, with the inorganic components in Clay A and Clay C very similar but different to those in Clay B. The variations in the clay characteristics have the potential to impact the performance of the clays when applied in their function as tap-hole clay plugging material.

As the next steps, additional sample characterisation tests will include X-ray tomography of the clays to quantify the porosity before and after heating, and to study the morphology of the pores. Development of methods to study workability, and wear mechanisms of the clays due to ferrochrome alloy and slag is currently underway at Mintek. Development of methods to study the sinterability and drillability of tap-hole clays will be useful. The performance of the clays in the aforementioned functions, will be presented relative to the clay characteristics presented in this study.

Acknowledgements

The paper is published with the permission of Mintek. The authors would like to thank their colleagues at Mintek for their assistance.

References

ASTM-D3172. 2013. Standard Practice for Proximate Analyses of Coal and Coke. West Conshohocken, PA, 2003: ASTM International.

ASTM-D3173. 2011. Standard Test Method for Moisture in the Analyses Sample of Coal and Coke. West Conshohocken, PA, 2003: ASTM International.

ASTM-D3174. 2012. Standard Test Method for Ash in the Analyses Sample of Coal and Coke from Coal. West Conshohocken, PA, 2003: ASTM International.

ASTM-D3175. 2011. Standard Test Method for Volatile Matter in the Analyses Sample of Coal and Coke. West Conshohocken, PA, 2003: ASTM International.

Dash, S.R. 2009. “Development of Improved Tap Hole Clay for Blast Furnace Tap Hole.” National Institute of Technology, Rourkela.

Guggenheim, S., and Martin R.T. 1995. “Definition of Clay and Clay Mineral: Joint Report of the AIPEA Nomenclature and CMS Nomenclature Committees.” Clays and Clay Minerals, Vol. 43, 255–56.

Heckroodt, R.O. 1991. "Clay and Clay Materials in South Africa." Journal of The Southern African Institute of Mining and Metallurgy 91 (10): 343–63.

Nelson, L.R., and Hundermark R.J. 2014. "'The Tap-Hole'' – Key to Furnace Performance.'" In Furnace Tapping 2014 Conference, 1–32. Muldersdrift, South Africa: The South African Institute of Mining and Metallurgy.

Nightingale, S., Wells L., Tanzil F.W.B.U., Cummins J., and Monaghan B.M. 2006. "Assessment of the Structural Development of Resin Bonded Taphole Clay (ICSTI 06)." In International Conference on the Science and Technology of Ironmaking, 251–55. Osaka, Japan: ISIJ.

Schulze, D.G. 2005. "Clay Minerals." Vol. 1, 246-254. Encyclopedia of Soils in the Environment, Elsevier / Academic Press, Boston.

Steenkamp, J.D, Mnisi M., and Skjeldstad A. 2018. "The Workability Index of Three Tap-Hole Clays." In , 1–13. Cape Town, South Africa: The Southern African Institute of Mining and Metallurgy.